Catal Lett (2010) 139:50–55
DOI 10.1007/s10562-010-0391-3

Mesostructured or Alumina-mesostructured Silica SBA-16 as Potential Support for NO_x Reduction and Ethanol Oxidation

Maya Boutros · Thomas Onfroy · Patrick Da Costa

Received: 6 February 2010 / Accepted: 4 June 2010 / Published online: 22 June 2010

Abstract The synthesis of some mesostructured silica or aluminosilica SBA-16 and Al-SBA-16 with 3D cubic structure is reported in this paper. The structural and porosity properties of these materials were studied by XRD, N_2 sorption and TEM imaging; the Al insertion was determined by ^{27}Al-MAS-NMR and acidic properties were characterized by pyridine adsorption followed by FT-IR spectroscopy. These solids were tested in the selective catalytic reduction of NO_x by ethanol in the presence of O_2. Compared to hexagonal mesoporous silica or aluminosilica (SBA-15 and Al-SBA-15), SBA-16 type materials (SBA-16 and Al-SBA-16) could be used as potential catalyst for the oxidation reaction and the SBA-16 solid has higher catalytic properties for the reduction of NO_x to N_2 at high temperature.

Keywords Mesoporous silica or aluminosilica · SBA-15 · SBA-16 · SCR NO_x · Ethanol · Pyridine

M. Boutros
Faculté des sciences II, Laboratoire de Chimie Physique des Matériaux (LCPM), Université Libanaise, Campus Fanar, BP 90656, Jdeideh, Lebanon

T. Onfroy
UPMC Univ Paris 06, CNRSFRE 3230, Laboratoire de Réactivité de Surface, Case 178, 4, Place Jussieu, 75252 Paris Cedex 05, France

P. Da Costa (✉)
Laboratoire Réactivité de Surface, UMR CNRS 7197, Université Pierre et Marie Curie, UPMC Paris 6, Université Pierre et Marie Curie, Case178, 4 Place Jussieu, 75252 Paris 05, France
e-mail: patrick.da_costa@upmc.fr

1 Introduction

The reduction of nitrogen oxides (NO_x) in a lean exhaust gases has become one of the most important environmental concerns in present times. Among them, nitrogen oxides (NO_x) are not only harmful for human beings but also contribute to environmental pollution by formation of acid rains, increasing the green-house effect, and participating in the formation of photochemical smog [1]. The removal of NO_x in the oxygen-rich exhausts demands a novel catalyst for a selective catalytic reduction (SCR) of NO_x. The SCR of NO_x by ammonia, or in some cases, urea, has become a fairly mature technology for stationary applications [2–4]. This technology is not so easy to implement on automotive field due to difficulties of storing and handling of NH_3. Selective Catalytic Reduction by Hydrocarbons (HC-SCR) is a process quite more attractive for NO_x abatement [5, 6]. Similarly, SCR of NO_x by alcohols (ethanol), seems to be interesting and acceptable for environmental purposes.

Up to now, multifarious catalysts such as zeolitic oxide, based on oxide/metals have been found to be effective for NO_x reduction in the presence of excess oxygen systems [7]. Mesoporous silicas have been also consider as an ideal solid supports due to their uniform/large pores, tunable pore sizes, high surface areas and a large number of highly dispersed active sites (the hydroxyl groups) on the pore walls and surface [8]. These solids should have a favorable impact on catalytic activity in comparison with microporous materials such as zeolites [9, 10]; microporous systems may have accessibility problems for gas molecules because diffusion in these small pore systems may affect adsorption equilibrium. Thus, to decrease the influence of diffusion effects it can be of interest to use mesoporous systems [11].

A family of highly ordered mesoporous silica materials (SBA acronym), with pores between 2 and 30 nm, has been synthesized using cationic alkylammonium surfactants [12], non ionic alkyl poly(ethylene oxide) oligomeric surfactants or poly(alkene oxide) triblock [13, 14]. Among them, the compounds SBA-15 and SBA-16, exhibiting arrangements of mesopores, respectively with 2D hexagonal (P6mm) and 3D cubic (Im3m) symmetry, have received particular attention [13]. SBA-15 mesoporous solids synthesized under acidic conditions exhibit larger pore size and higher pore volume wall compared to M41S. The improved hydrothermal and thermal stability makes them promising catalytic materials [13]. The introduction of Al into the structure of SBA-15 is an effective way to enhance the acidity, which may promotes the SCR reactions [15, 16]. The structural characteristics of SBA-16 make it an interesting material for catalysis applications [17], the insertion of a metal ion, such as aluminium, in the silica framwork SBA-16 solid is desired.

The aim of this present paper is to compare SBA-15 and SBA-16 in order to recognize the influence of mesoporous materials on the catalytic activity for the Selective Catalytic Reduction of NO_x by ethanol in Lean Burn Conditions.

We studied, for the first time, the synthesis of the mesostructured silica and aluminosilica samples SBA-16 and Al-SBA-16 with a 3D cubic arrangement of mesopores. These solids were characterised by X ray diffraction, N_2 sorption, Transmission Electronic Microscopy (TEM), ^{27}Al-MAS-NMR, pyridine adsorption followed by FT-IR spectroscopy, tested in SCR NO_x and compared to 2D hexagonal mesoporous materials (SBA-15 and Al-SBA-15).

2 Experimental

2.1 Mesoporous SBA-16 and Al-SBA-16 Materials Synthesis

a) The mesoporous SBA-16 silica was synthesized according to the method reported by Shen et al. [18]. In detail, 4.0 g of triblock copolymer F127 ($(EO)_{20}(PO)_{70}(EO)_{20}$, M_{av} = 12600, Sigma) were dissolved at 40 °C in 125 mL of a HCl solution (2 mol L^{-1}) under magnetic stirring to obtain a homogeneous solution. Then, 8.5 g of tetraethyl orthosilicate (TEOS, ≥99%, Fluka) were added to the acidic solution. The mixture solution was further stirred for 24 h at 30 °C and then placed in a Teflon bottle and heated to 80 °C for 24 h. The as-synthesized mesoporous composite was filtered and dried in the air. Template free products were obtained by calcination the as-synthesized sample in air at 550 °C for 6 h.

b) To prepare the mesostrutured SBA-16-related aluminosilicate, we adapted the pH-adjusting method proposed in the literature by Gallo et al. [19]. Al-SBA-16 sample was prepared by dissolving 4.0 g of F127 and 125 mL of HCl 2 mol L^{-1}, the solution were stirred for 15 h at 35 °C. Then, 8.5 g of TEOS were added, the mixture was stirred for 4 h and 0.88 g of aluminium isopropoxyde ($Al[(CH_3)_2CHO)]_3$, 98%, Aldrich) (Si/Al = 10) were added. After 20 h of stirring at 35 °C, the white dispersion was transferred to an autoclave for hydrothermal treatment at 100 °C for 24 h. After a pH adjustment at 7.5 with concentrated ammonium hydroxide solution (30 wt%, NH_3, Carlo/Erba), the dispersion was treated for another 24 h at the same temperature as it was mentioned previously.

Finally, the sample was filtered, washed with water and calcined two times at 550 °C for 6 h.

2.2 Mesoporous SBA-15 and Al-SBA-15 Materials Synthesis

Pure silica SBA-15 and aluminosilica Al-SBA-15 (Si/Al = 10) were synthesized using a hydrthermal method described by Zhao et al. [13] and Li et al. [20], respectively. We reported in details the synthesis of SBA-15 and Al-SBA-15 solids in reference [21].

2.3 Catalyst Characterization

Aluminium and silicon composition of the various materials were determined by elemental analysis (ICPAES) in the CNRS center at Vernaison (France).

XRD data were recorded on a Bruker Advanced D8 using CuKα radiation. PXRD measurements were performed from 0.5 to 5° (2θ) in steps of 0.02° with a count time of 6 s at each point. N_2 adsorption–desorption isotherms were measured at liquid nitrogen temperature by a Micromeritics ASAP 2010. Before the measurements, the samples were evacuated at 200 °C under vacuum (2.10^{-3} Torr). The pore diameter and specific pore volume were calculated according to the Barrett–Joyner–Halenda (BJH) model. The specific surface area was obtained by using the Brunauer–Emmett–Teller (BET) equation.

High resolution TEM (HRTEM) was performed on a JEOL-JEM 2011 h (LaB) microscope operating at 200 kV.

Nuclear magnetic resonance of ^{27}Al with magic-angle spinning spectra was performed in a BRUKER AVANCE 400 spectrometer (9.4 T) operating at 104.5 MHz. The samples were confined in a 4 mm zirconia rotor spinning at 10 kHz.

IR spectra were recorded with a Bruker Vector 22 FT-IR spectrometer (resolution: 4 cm^{-1}). Samples were pressed into discs ($\sim$5 mg/cm^2) and activated at 400 °C for 2 h in

O_2 ($P_{equilibrium}$ = 13.3 kPa), and finally evacuated for 1 h at the same temperature. The acidic properties (type and abundance) of the samples were monitored by the use of pyridine. Pyridine was introduced at R.T. (P = 133 Pa) followed by thermal desorption from 150 to 350 °C. The abundance of Brønsted and Lewis acid sites was calculated using the integrated molar absorption coefficient values determined by Emeis et al. [22] (i.e. 1.67 cm μmol^{-1} for the ν_{19b} vibration of protonated pyridine at $\sim$1448 cm^{-1} and 2.2 cm μmol^{-1} for the ν_{19b} vibration of coordinated pyridine at $\sim$1447 cm^{-1}).

2.4 Catalytic Measurements

Temperature-programmed surface reaction (TPSR) and steady state experiments were carried, in a U-type glass reactor by using gas mixture consisting of 500 ppm NO + 2500 ppm C_2H_5OH + 10% O_2 in Ar. The gases (NO, O_2 and Ar) were fed from compressed cylinders provided by Air Liquide and adjusted with Brooks mass flow controllers (5850 TR and 5850 TE). Ethanol was supplied to the reacting stream by means of two temperature-controlled bubble towers (purged by Ar flow): a saturator at RT and a condenser at −5 °C. The total flow rate of the feed gas was maintained at 250 mL min^{-1}. The sample (90 mg) was held on plugs of quartz wool and the temperature was controlled through a EUROTHERM 2408 temperature controller, K-type thermocouple. The outflow experimental reaction was continuously monitored a variety of detectors such as: An Eco Physics CLD 700 AL chemiluminescence NO_x analyser (for NO and total NO_x (i.e. NO + NO_2), which allowed the simultaneous detection of NO and NO_x. Two Ultramat 6 IR analysers were used to monitor N_2O, CO and CO_2. A FID detector (Fidamat 5) was used to follow the concentration of the hydrocarbonated compounds.

3 Results and Discussion

3.1 Characterization of the Mesostrutured Samples

As shown in Fig. 1, calcined pure silica SBA-16 templated with tri-block polymer F127 exhibited a well-resolved XRD pattern with a sharp diffraction peak at 2 θ = 0.82° and two latter overlapped at 1.1° and 1.2°. The three diffractions peaks can further been indexed as 110, 200, 211, in which a typical characteristic pattern with cubic Im3m mesostructure was determined.

In the case of aluminium containing material (Al-SBA-16, Fig. 1 curve b), only the peak indexed as [110] is slowly observed, probably because the aluminium insertion leads to a structure with lower order. The pores width

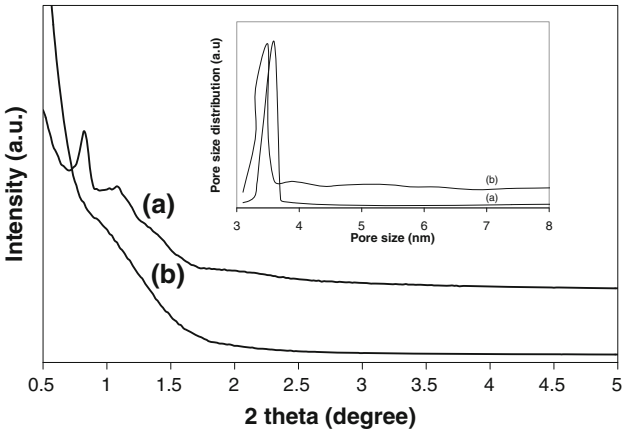

Fig. 1 X-ray diffraction patterns of (*a*) SBA-16 and (*b*) Al-SBA-16 [Inset: Pore size distribution curves of (*a*) SBA-16 and (*b*) Al-SBA-16]

distribution with a maximum of 3.2 and 3.6 nm were found for SBA-16 and Al-SBA-16, respectively. These solids have the same textural properties as those reported in the literature. [19, 23].

The calcined SBA-16 and Al-SBA-16 samples presents a type IV nitrogen adsorption isotherm (Figures not shown) with a hysteresis loop, commonly observed for mesoporous materials [23].

The TEM image of Al-SBA-16 material shows a silica with an ordered architecture of mesopores channels (Fig. 2), the channels still structured in the case of alumina-mesostructured sample that despite the introduction of aluminium in the synthesis gel.

Both, SBA-15 and Al-SBA-15, have similar patterns with three well-resolved characteristic diffraction peaks wich are attributed to 100, 110 and 200 in the hexagonal structure. The X-ray diffraction of these two samples are presented in a prelimineray study decsribed by Boutros et al. in the reference [21].

For Al-SBA-15 and Al-SBA-16 materials, aluminum insertion through the co-condensation technique was partial (Si/Al obtained is 13 instead of 10). The larger surface

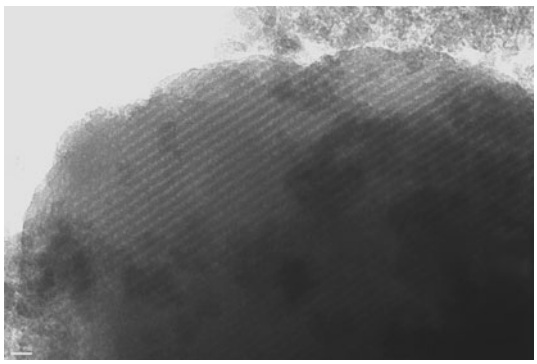

Fig. 2 TEM image of Al-SBA-16

area ($\sim$900 m^2 g^{-1}) of the SBA-16 is related to a substantial contribution of porosity in the range of 1 and 3 nm, which are almost absent in the Al-containing material [19]. The inclusion of aluminum into the structure of SBA-16 conducted to a large modification of the specific surface area (−66%) that is not the case of hexagonal mesoporous aluminosilica sample

Al-SBA-15 (Table 1). This is an argument with less ordered structure of Al-SBA-16 detected by XRD.

^{27}Al-MAS-NMR is well known to give useful information that enables to ascertain the presence of tetra, penta and octa coordinated Al species in various alumino-silicates like zeolite and mesoporous materials. Figure 3 shows the ^{27}Al-MAS-NMR spectra of aluminium containing mesoporous materials.

For Al-SBA-15 solid (Fig. 3b), the spectra give two resolved lines at 53 and $\sim$0 ppm. The line at 53 ppm can be assigned to aluminum in a tetrahedral environment (AlO_4, structural unit, Al(tet)), in which aluminum is covalently bound to four framework Si atoms via oxygen bridges. The chemical shift at 0 ppm can be assigned to octahedral extra framework aluminum (AlO_6 structural unit, Al(oct)) [24]. Yue et al. [25] reported the presence of penta coordinated Al in Al-SBA-15 material synthesized by this direct method. A separate peak for penta coordinated Al is not noticed, however, its presence in minor amounts can not be ruled out by considering the broadness of the 53 ppm peak especially at low Al content [26]. The results indicated that under our synthesis conditions a part of Al is incorporated into the SBA-15 structure, although some non-framework Al is consistently present in our results.

The insertion of aluminium in the silica framework SBA-16 was determined by ^{27}Al-MAS-NMR (Fig. 3a). Signals at approximately 0 and 49 ppm, respectively, due to octahedral and tetrahedral Al were detected.

Comparing the two aluminosilicate samples, one can see that, the peak at $\sim$50 ppm is more intense in the case of Al-SBA-15. The percentage of tetraedral framework Al species is higher in the hexagonal mesoporous than the cubic mesostrutured aluminosilica samples. This results indicate that a lower proportion of aluminium is incorportated into SBA-16 framework than SBA-15.

Acidic properties of Al-SBA-15 and Al-SBA-16 were monitored by pyridine adsorption–desorption followed by infrared spectroscopy. Spectra of adsorbed pyridine at 150 (Fig. 4) and 250 °C (not shown) exhibit four bands at 1624, 1578, 1496 and 1456 cm^{-1} which can be attributed to pyridine coordinatively bound to Lewis acid sites [27] and two others at 1640 and 1546 cm^{-1} related to pyridinium species [27]. With increasing desorption temperature to 350 °C, only Lewis acid sites are observed which indicates that Brønsted acid sites are not strong enough to retain pyridine at high temperature. Although, the two studied samples present strong Lewis acid sites characterized by the band at 1624 cm^{-1} which is attributed to pyridine adsorbed on coordinatively unsaturated Al in tetrahedral environment [27]. According to Table 2, the amount of Brønsted acid sites is between 2.3 (at 150 °C) and 1.6 (at 250 °C) time higher on Al-SBA-15 than in Al-SBA-16 and

Table 1 Textural properties of the mesostructured samples

Samples	S_{BET} (m^2 g^{-1})	V_{pores} (cm^3 g^{-1})	D_{pores} (nm)
Si-SBA-16	935	0.84	3.6
Al-SBA-16	317	0.86	3.5
Si-SBA-15	972	1.04	7.1
Al-SBA-15	818	1.1	8.2

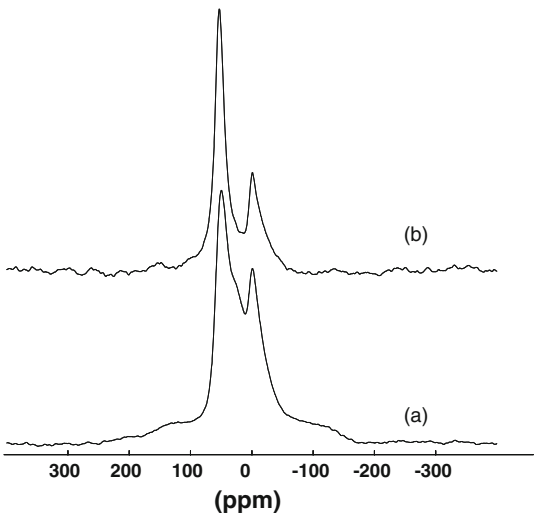

Fig. 3 ^{27}Al-MAS-NMR of (*a*) Al-SBA-16 and (*b*) Al-SBA-15

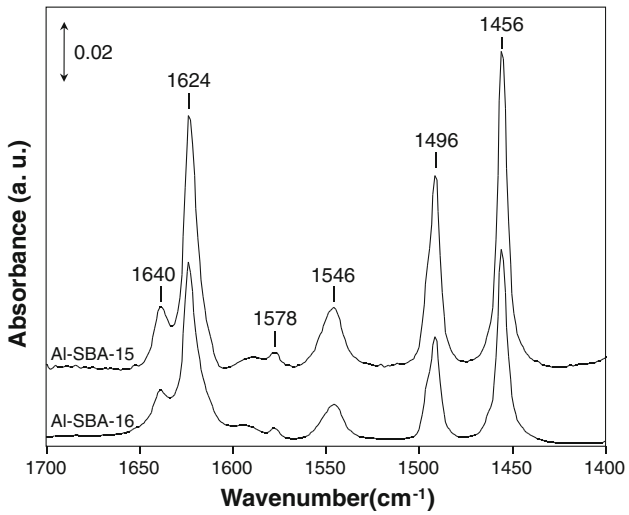

Fig. 4 FTIR spectra of Al-SBA-15 and Al-SBA-16 catalysts after pyridine desorption at 150 °C

Table 2 Acidic properties of the mesostructured samples

Samples	Brønsted acid sites (μmol g^{-1})			Lewis acid sites (μmol g^{-1})		
	150°	250°	350°	150°	250°	350°
Al-SBA-15	44	7	0	128	89	54
Al-SBA-16	19	2	0	60	40	24

the amount of Lewis acid sites is 2.2 time higher on Al-SBA-15 and thus whatever the desorption temperature.

3.2 SCR of NO_x by Ethanol

It is clear that NO previous work have been done on SBA-16 based materials as a catalyst for SCR deNOx applications using ethanol as reducing agent.

Selective reduction of NO_x runs, in presence of mesoporous silica or aluminosilica materials, were carried out using the following feed: 500 ppm NO + 2500 ppm C_2H_5OH + 10% O_2 in Ar. NO_x conversion as function of temperature is presented in Fig. 5. In all experiments, no N_2O was detected and only nitrogen was observed as product.

First, we compared the catalytic activity of cubic mesostructured samples SBA-16 and Al-SBA-16 in the reduction of NO_x by ethanol (Fig. 5). The SBA-16 solid remains more active at high temperature. The maximum of conversion of NO_x to N_2 is less to 60% at 500 °C. For Al-SBA-16 sample obtained by direct hydrothermal synthesis, we analyzed that the insertion of aluminum into the structure of SBA-16 mesoporous silica enhances the activity at low temperature (<350 °C) but the conversion of NO_x to N_2 decrease significantly, when the temperature was increased. This is probably related to the less ordered structure and the lower specific surface area of this sample relative to the support SBA-16 determined, respectively by X-ray diffraction and N_2 adsorption–desorption. Figure 6 shows the conversion of ethanol oxidation into CO and CO_2 as function of temperature. The Al-SBA-16 is more active than the pure mesoporous cubic silica SBA-16, over the range of temperature.

Moreover, in the case of 2D hexagonal mesoporous solid, according with the literature, the insertion of aluminum into the structure of SBA-15 enhances its acidity and promotes the SCR reaction. The Al-SBA-15 sample is more active in the NO_x conversion than the pure SBA-15 silica, especially at high temperatures.

The pure silica SBA-16 remains the best catalyst for the SCR NO_x at high temperature. However, comparing the aluminum containing mesostructured samples Al-SBA-16 and Al-SBA-15 with the same percentage of aluminum, the solid with 2D hexagonal structure (Al-SBA-15) is more active in the NO_x conversion than this one with 3D cubic arrangement of mesopores (Al-SBA-16). In order to understand the difference in the catalytic activity, some parameters should be mentioned: (i) The tetrahedral framework aluminum species enhances the N_2 selectivity and (ii) the acidic properties and especially the Lewis acid sites increase the activity of catalysts in the deNO_x reaction.

Finally, we can note that the cubic SBA-16 sample has a higher capability as a catalyst oxidation than the hexagonal SBA-15 solid, in which the Al-SBA-16 leads to a better oxidation of ethanol into CO and CO_2 ($\sim$70% at 450 °C, Fig. 6).

4 Conclusion

Aluminium containing 3D cubic mesostructured material was obtained by modification of the synthesis of pure SBA-

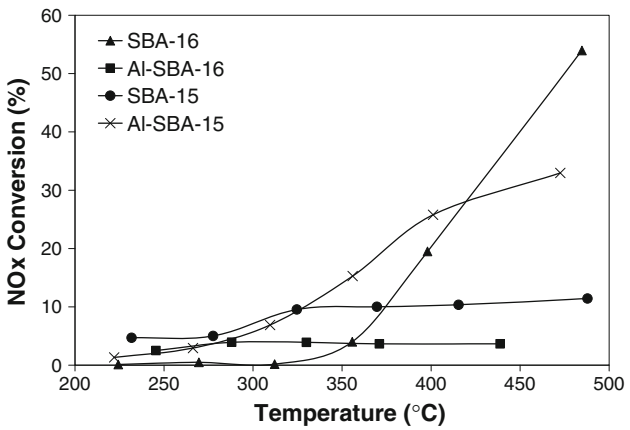

Fig. 5 Steady state NO_x conversion as function of temperature for the mesostructured samples

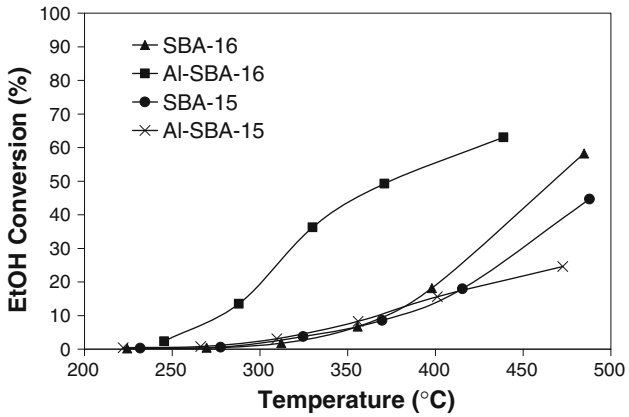

Fig. 6 Steady-state EtOH conversion into CO and CO_2 as function of temperature for the mesostructured samples

16 silica and compared to hexagonal mesoporous solids (SBA-15 and Al-SBA-15). The ^{27}Al-MAS-NMR results indicate that a lower proportion of aluminium is incorporated into SBA-16 framework than SBA-15. Pyridine adsorption–desorption followed by infrared spectroscopy shows that Brønsted and Lewis acid sites remains more higher in Al-SBA-15 compared to Al-SBA-16.

The cubic mesoporous sample, were used, for the first time, as catalysts in the reduction of NO_x to N_2 using ethanol as reducing agent. SBA-16 catalyst converted as much as 50% NO_x to N_2 at high temperature in Lean Burn Conditions. The insertion of aluminium in this sample decrease the catalytic activity compared with other active phases such as Al-SBA-15. It is seen that ethanol has higher oxidant characteristic in the presence of Al-SBA-16 sample. The catalytic performance of these mesoporous materials stongly depended on the hexagonal or cubic structure, the octaedral or tetraedral aluminium species and finally on the acidic properties.

Acknowledgment The authors thank M. Charles Corredor from *Grove School of Engineering- City College of New York.*

References

1. Musi A, Massiani P, Brouri D, Trichard J-M, Da Costa P (2009) Catal Lett 128:25
2. Nakajima F (1991) Catal Today 10:1
3. Fritz A, Pitchon V (1997) Appl Catal B 13:1
4. Heck RM (1999) Catal Today 53:519
5. Armor JN (1995) Catal Today 26:99
6. Iwamato M (1996) Catal Today 29:29
7. Burch R, Breen JP, Meunier FC (2002) Appl Catal B 39:283
8. Huang HY, Yang RT, Chinn D, Munson CL (2003) Ind Eng Chem Res 42:2427
9. Sayari A (1996) Chem Mater 8:1840
10. Corma A (1997) Chem Rev 97:2373
11. Knôfel C, Descarpentries J, Benzaouia A, Zeleňák V, Mornet S, Llewellyn PL, Hornebecq V (2007) Microporous Mesoporous Mater 99:79
12. Huo Q, Margolese DI, Ciesla U, Demuth DG, Feng P, Gier TE, Sieger P, Firouzi A, Chmelka BF, Schüth F, Stucky GD (1994) Chem Mater 6:1176
13. Zhao D, Huo Q, Feng J, Chmelka F, Stucky GD (1998) J Am Chem Soc 120:6024
14. Huo Q, Margolese DI, Stucky GD (1996) Chem Mater 8:1147
15. Linag X, Li J, Lin Q, Sun K (2007) Catal Commun 8:1901
16. Brandhorst M, Zajac J, Jones DJ, Rosière J, Womes M, Jimenez-López A, Rodríguez-Castellón E (2005) Appl Catal B 55:267
17. Wu S, Han Y, Zou YC, Song JW, Zhao L, Di Y, Liu SZ, Xiao FS (2004) Chem Mater 16:486
18. Shen S, Deng Y, Zhu G, Mao D, Wang Y, Wu G, Li J, Liu X, Lu G, Zhao D (2007) J Mater Sci 42:7057
19. Gallo JMR, Bisio C, Marchese L, Pastore HO (2008) Microporous Mesoporous Mater 111:632
20. Li Y, Zhang W, Yang Q, Wie Z (2004) J Phys Chem B 108:9739
21. Boutros M, Trichard JM, Da Costa P (2009) Appl Catal B 91:640
22. Emeis CA (1993) J Catal 141:347
23. Aburto J, Ayala M, Bustos-Jaims I, Montiel C, Terres E, Dommnguez JM, Torres E (2005) Microporous Mesoporous Mater 83:578
24. Nie C, Huang L, Zhao D, Li Q (2001) Catal Lett 71:117
25. Yue Y-H, Gedeon A, Bonardet J-L, d'Espinose JB, Melosh N, Fraissard J (2000) Stud Surf Sci Catal 129:209
26. Kumaran GM, Garg S, Soni K, Kumar M, Gupta JK, Sharma LD, Rama Rao KS, Murali Dhar G (2008) Microporous Mesoporous Mater 114:103
27. Morterra C, Magnacca G (1996) Catal Today 27:497